Remote Sensing of Environment 145 (2014) 25–37

Contents lists available at ScienceDirect

Remote Sensing of Environment

journal homepage: www.elsevier.com/locate/rse

Retrieval of leaf area index using temporal, spectral, and angular information from multiple satellite data

Qiang Liu [a,*], Shunlin Liang [a,b], Zhiqiang Xiao [c], Hongliang Fang [d]

[a] State Key Laboratory of Remote Sensing Science, College of Global Change and Earth System Science, Beijing Normal University, Beijing 100875, China
[b] Department of Geographical Sciences, University of Maryland, College Park, MD 20742, USA
[c] State Key Laboratory of Remote Sensing Science, School of Geography, Beijing Normal University, Beijing 100875, China
[d] LREIS, Institute of Geographic Sciences and Natural Resources Research, Chinese Academy of Sciences, Beijing 100101, China

ARTICLE INFO

Article history:
Received 19 June 2013
Received in revised form 9 November 2013
Accepted 28 January 2014
Available online 22 February 2014

Keywords:
Leaf area index
Multiple sensors
Ensemble Kalman filter
Iterative method

ABSTRACT

The leaf area index (LAI) is one of the most critical structural parameters of the vegetation canopy in regional and global biogeochemical, ecological, and meteorological applications. Data gaps and spatial and temporal inconsistencies exist in most of the existing global LAI products derived from single-satellite data because of their limited information content. Furthermore, the accuracy of current LAI products may not meet the requirements of certain applications. Therefore, LAI retrieval from multiple satellite data is becoming popular. An existing LAI inversion scheme using the ensemble Kalman filter (EnKF) technique is further extended in this study to integrate temporal, spectral, and angular information from Moderate Resolution Imaging Spectroradiometer (MODIS), SPOT/VEGETATION, and Multi-angle Imaging Spectroradiometer (MISR) data. The recursive update of LAI climatology with the retrieved LAI and the coupling of a canopy radiative-transfer model and a dynamic process model using the EnKF technique can fill in missing data and produce a consistent accurate time-series LAI product. During each iteration, we defined a $5 * 1$ sliding window and compared the RMSEs in the selected window to determine the minimum. Validation results at six sites demonstrate that the combination of temporal information from multiple sensors, spectral information provided by red and near-infrared (NIR) bands, and angular information from MISR bidirectional reflectance factor (BRF) data can provide a more accurate estimate of LAI than previously available.

1. Introduction

The booming development of land-surface ecosystems modeling and environmental monitoring techniques has resulted in an urgent demand for high-quality, long-term consistent biophysical parameters. Leaf area index (LAI), defined as one half of the total leaf surface area per unit horizontal ground surface area (Chen & Black, 1992) , measures the amount of leaf material in an ecosystem, which imposes important controls on photosynthesis, respiration, rain interception, and other processes (GTOS, 2007). Consequently, LAI is a key variable that couples vegetation to the modeling of ecosystem productivity (Running et al., 1999; Zhang, Anderson, Tan, Huang, & Myneni, 2005), energy, and mass exchange between the land surface and the atmosphere (Bonan, 1995; Dickinson, 1995; Nouvellon et al., 2000; Sellers et al., 1997). Currently, two approaches are widely used to retrieve LAI from satellite data (Liang, 2007). The first uses empirical or semi-empirical statistical relationships between LAI and spectral vegetation indices (Baret & Guyot, 1991; Liang, 2004; Myneni, Hall, Sellers, & Marshak, 1995; Wang, Huang, Tang, & Wang, 2007). Vegetation indices are designed as a combination of surface reflectance to maximize information about canopy characteristics and minimize interference factors from the atmosphere and soil. The second approach is the inversion of a radiative-transfer model that simulates surface reflectance from canopy structure parameters (e.g., LAI), soil, leaf optical properties, and view-illumination geometry (Myneni, Nemani, & Running, 1997; Xiao, Liang, Wang, Song, & Wu, 2009). Moreover, simulated lookup tables (LUTs) (Knyazikhin, Martonchik, Myneni, Diner, & Running, 1998; Shabanov et al., 2005) and trained neural networks (NNs) (Bacour, Baret, Béal, Weiss, & Pavageau, 2006; Fang & Liang, 2003a; Walthalla et al., 2004) are commonly used to simplify the process of deriving radiative-transfer models and to improve the efficiency of inversion.

Several LAI products have been derived from various sets of satellite observation data using the above three approaches over regional to global domains. NOAA/AVHRR is the early moderate resolution sensor used to produce global LAI values at 0.25° spatial sampling and a monthly time cycle (Buermann, Dong, Zeng, Myneni, & Dickinson, 2001; Los et al., 2000; Myneni et al., 1997; Sellers et al., 1996) and ECOCLIMAP LAI (Masson, Champeaux, Chauvin, Meriguer, & Lacaze, 2003) at

* Corresponding author at: State Key Laboratory of Remote Sensing Science,College of Global Change and Earth System Science, Beijing Normal University, Beijing, 100875, China.
E-mail address: liuqiangrs2007@gmail.com (Q. Liu).

http://dx.doi.org/10.1016/j.rse.2014.01.021
0034-4257/

1/120° spatial sampling and the same time cycle as AVHRR LAI.CYCLOPES (Baret et al., 2007). GLOBCARBON (Deng, Chen, Plummer, Chen, & Pisek, 2006) and a CCRS regional product (Fernandes, Butson, Leblanc, & Latifovic, 2003) have been derived from SPOT/VEGETATION since 1998. Their spatial resolutions are 1/112°, 1/11.2°, and 1 km respectively; the temporal resolution of CYCLOPES and CCRS is 10 days, while that of GLOBCARBON is one month. A widely used eight-day synthesized LAI product has been generated from Terra-Aqua/MODIS at 1 km spatial resolution since 2000 (Knyazikhin et al., 1998; Yang et al., 2006). The Langley Atmospheric Sciences Data Center (ASDC) has been routinely processing a LAI product from MISR data since October 2002 (Diner et al., 1999). Recently, a Global Land Surface Satellite (GLASS) LAI product with 5/1 km spatial resolution and an eight-day temporal sampling period was generated from time-series AVHRR/MODIS reflectance data using general regression neural networks (Xiao et al., 2013). Other global LAI data sets produced from ADEOS/POLDER (Roujean & Lacaze, 2002), ENVISAT/MERIS (Bacour et al., 2006), and MSG/SEVIRI (García-Haro, Coca, & Miralles, 2008) are restricted by time period or spatial coverage.

Validation campaigns aimed at improving the understanding of these satellite LAI products for users and developers are ongoing. Current research has revealed that the uncertainties of typical LAI products such as MODIS, CYCLOPES (Fang, Wei, & Liang, 2012), MISR (Hu et al., 2007), GLOBCARBON, and ECOCLIMAP (Garrigues, Lacaze, et al., 2008) are still unable to meet the target accuracy of ± 0.5 according to the Global Climate Observation System (GCOS) requirement (GCOS, 2006). Furthermore, LAI data gaps and inconsistencies existing in these products may also restrict their application (Wang, 2012; Xiao, 2012).

Most of the LAI products mentioned above are generated from single-satellite observation data; the limited amount of information in the retrieval process accounts for the appearance of data gaps and inconsistencies, especially under poor observation conditions. Several attempts have been made to improve the quality of LAI data. One way is to develop complex algorithms based on physical principles and integrating various sources of prior information. Combal et al. (2002) used prior information to solve the ill-posed inverse problem of canopy biophysical variable retrieval. Koetz, Baret, Poilvé, and Hill (2005) used coupled canopy structure dynamic and radiative-transfer models to estimate biophysical canopy characteristics. Another approach is to integrate remotely sensed information from multiple satellite data sets into the retrieval process. Gonsamo and Chen (2014) incorporated background, topography, and foliage clumping information to improve the University of Toronto (UofT) LAI algorithm. Ganguly et al. (2008) developed a multi-sensor retrieval algorithm to derive LAI and FAPAR products from the Advanced Very High Resolution Radiometer (AVHRR), which demonstrated the effectiveness of more measured information (spectral and/or angular variation). Gray and Song (2012) developed a novel approach for mapping effective LAI using spectral information from Landsat, spatial information from IKONOS, and temporal information from MODIS.

Xiao, Liang, Wang, and Jiang (2011) developed coupled dynamic and radiative-transfer models to estimate real-time LAI from MODIS time-series data. This approach is able to fill in gaps and to provide better accuracy. However, it is based on MODIS data alone. In this study, this method has been further extended to integrate multiple satellite data with various sets of temporal, spectral, and angular information to improve accuracy, fill in gaps, and eliminate inconsistencies. Moreover, the practice of using the retrieved LAI as prior information to update the dynamic model was demonstrated to be beneficial to the further development of inversion. The following sections present the detailed methodology, validation results, discussion, and conclusions.

2. Methodology

The basic procedure of the extended method is briefly illustrated in Fig. 1. The combination of time-series MODIS, CYCLOPES, and MISR LAI data can minimize gaps and produce better LAI climatology because of the different observation cycles of multiple sensors. The LAI climatology works in the background using the assimilation method and the initial values to construct the dynamic model. High-quality, cloud-free land-surface reflectance data extracted from MODIS, SPOT/VEGETATION, and MISR are used to update the predictions of the dynamic model recursively with the help of the EnKF technique and the radiative-transfer model. The updated LAI is then used to improve the predictions of the dynamic model.

In the extended approach, an iterative method is proposed to improve retrieval accuracy. Retrieved LAI values are used to substitute for LAI climatology to provide better estimates for the dynamic model and the radiative-transfer model. The root mean square error (RMSE) between the retrieved LAI values and LAI climatology is used to measure the improvement in the retrieval process and determine exit criteria for the iterations. A decreasing RMSE with further iterations means that the LAI climatology is approaching the retrieved LAI values. In other words, the performance of the iterative procedure is declining, and therefore the procedure is terminated. In addition, this research has developed three progressive tests to assess the performance of temporal, spectral, and angular information in the retrieval process and to find out the best way to combine them. Data sets (including field measurements and remote sensing data) and critical components of this method are described in detail below.

2.1. Field measurement of LAI

Various validation studies have involved taking detailed field measurements of LAI using direct methods (e.g., destructive sampling) and indirect methods (e.g., LAI-2000, AccuPAR, Digital Hemispherical Photographs, etc.) (Garrigues, Shabanov, et al., 2008; Jonckheere et al., 2004; Weiss, Baret, Smith, Jonckheere, & Coppin, 2004). In the present study, LAI measurements for six sites were selected from existing research networks, including FluxNet (WWW1), AmeriFlux (WWW2), Bigfoot (Cohen & Justice, 1999), and VALERI (WWW3) (Baret et al., 2005), based on the principles of enough observations during the survey period and typical land-surface biomes. The biomes of the selected validation sites can be categorized into cropland, grassland, and forest. Basic information on the validation sites is listed in Table 1.

The Bondville site is an agricultural site in the Midwestern United States near Champaign, Illinois. The field was continuous no-till with alternating years of soybean and maize crops (Kuusk, 2001). The Rosemount-G19 AmeriFlux site is located within an exclusively agricultural landscape, and the type of agriculture is common among the upper Midwestern states of the United States. The Mead Irrigated site is located in Nebraska, United States, and the biome of this validation site is maize. Hainich contains the largest coherent area of deciduous trees in Germany. The dominant trees are beech, mixed with ash, maple, tilia cordata, hornbeam, and chequer tree. The Dahra North and Tessekre North sites are located close together in Africa and are both covered with sparse grass savanna. The field LAI measurements for these two sites were relatively lower than the others listed in Table 1 and were used to test the applicability of the proposed method, especially under conditions where background noise is obvious and the vegetation distribution is sparse.

The measurement method for the above validation sites was indirect except for Mead Irrigated and Bondville. The result of destructive sampling is true LAI, while the results of indirect methods (e.g., LAI-2000 and AccuPAR) are known as effective LAI because of the assumption of uniformly distributed leaves and ignorance of foliage clumping. To eliminate the effect of foliage clumping due to the indirect measurement methods described above, effective LAI measurements must be converted to true LAI. VALERI (WWW3) provides numerous measurements of effective LAI and the corresponding true LAI, enabling linear regression models based on specific biomes (e.g., cropland, grassland, and forest) to be built to perform conversion from effective LAI to true LAI

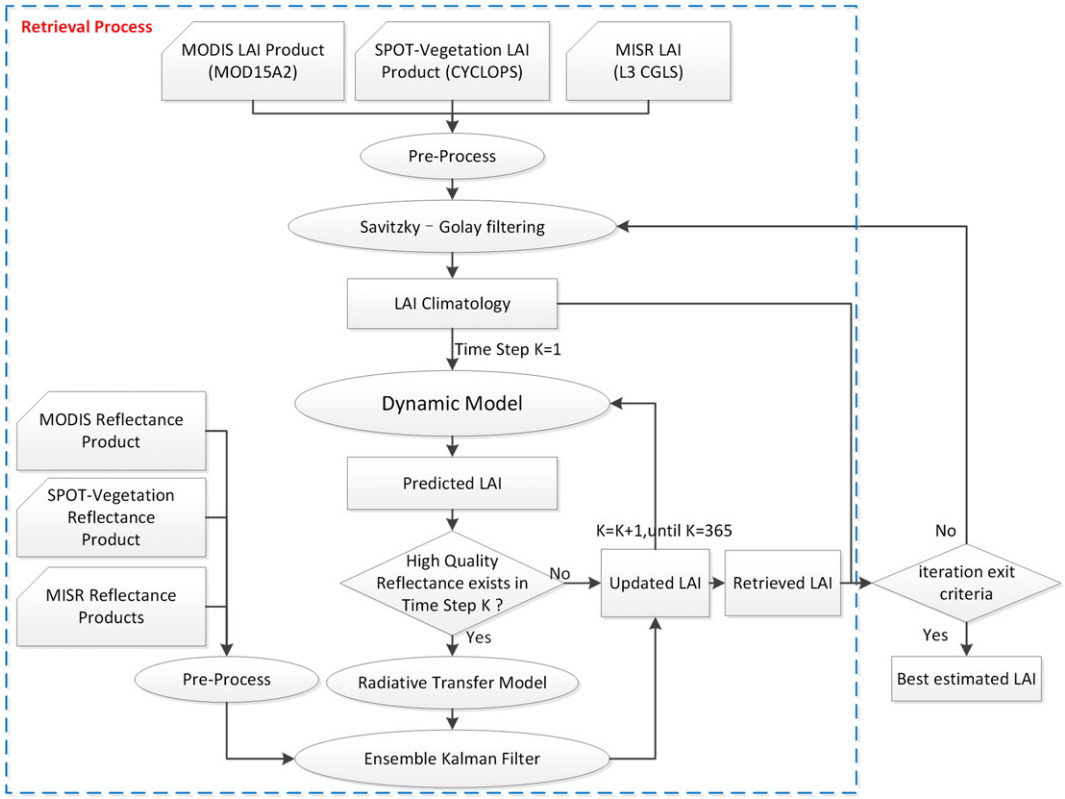

Fig. 1. Flowchart of an LAI inversion method using multiple sensors.

(Fig. 2). The linear regression model is highly reasonable, with R-squared no less than 0.92 and P-values less than 0.001.

2.2. Remote sensing data sets

To apply this extended method to the global scale in the next stage, we decided to choose LAI products with sufficient time period and spatial coverage. Hence, CCRS and other products from ADEOS/POLDER or MSG/SEVIRI were excluded from this research. Compared with the relatively higher spatial resolution of MODIS LAI (1 km) and CYCLOPES LAI (1/112°, approximately 1 km at the Equator in a *plate-carrée* projection), the GLOBCARBON LAI is coarse, with a pixel size of 1/11.2° (approximately 10 km at the Equator in a *plate-carrée* projection). Moreover, its temporal resolution (one month) is less than those of MODIS LAI (8 days) and CYCLOPES LAI (10 days). The MISR LAI product shows better structural variability (Hu et al., 2007) than other measures due to the specific observational approach used. Therefore, the inclusion of MISR data also provides the capability to improve the accuracy of surface characterization. Taking all these factors into consideration, we eventually used MODIS, MISR, and CYCLOPES LAI and their corresponding surface reflectance products in the proposed method. Table 2 shows the characteristics of the selected LAI products and their corresponding land-surface reflectance products used in this study.

MODIS, SPOT/VEGETATION, and MISR surface reflectance data are routinely used to generate global LAI products. The MODIS LAI product, available through NASA's Warehouse Inventory Search Tool (WIST) interface (WWW4), is derived from a main ($QC < 64$) and a backup ($64 \leq QC < 128$) algorithm according to an ancillary quality-control (QC) layer. The CYCLOPES LAI (V3.1) has been generated from SPOT/VEGETATION at a resolution of 1/112° every 10 days from 1999 to 2007. This measure can be downloaded from the POSTEL Land Surface Thematic Centre (WWW5). The status map (SM) layer is used to indicate data quality; $SM = 0$ indicates the best retrieval, while $SM > 0$ means that the retrieval is suboptimal due to potential aerosol, cloud, or snow contamination. The MISR LAI (WWW6) used in this paper is a Level 3 component global land-surface (CGLS) product which is summarized from the best LAI estimation of Level 2 land-surface data on the basis of an ancillary quality-assessment (QA) flag, meaning that it can be regarded as the finest level of LAI data.

Before integrating MODIS, SPOT/VEGETATION, and MISR data, it is necessary to minimize the influence of different spatial resolutions and projections. To match different observations geometrically, we used the General Cartographic Transformation Package software

Table 1
Basic information on the validation sites.

Site name	Latitude (°)	Longitude (°)	Measurement method	Biome type	Year(s)
Bondville	40.0061	−88.292	Destructive sampling	Croplands	2004, 2005, and 2006
Rosemount-G19	44.7217	−93.089	AccuPAR	Corn	2003
Mead Irrigated	41.1651	−96.477	Destructive sampling	Maize	2002
Hainich	51.0793	10.452	LAI-2000	Mixed forest	2001
Dahra North	15.3675	−15.443	LAI-2000	Grass savanna	2002
Tessekre North	15.896	−15.061	LAI-2000	Grass savanna	2002

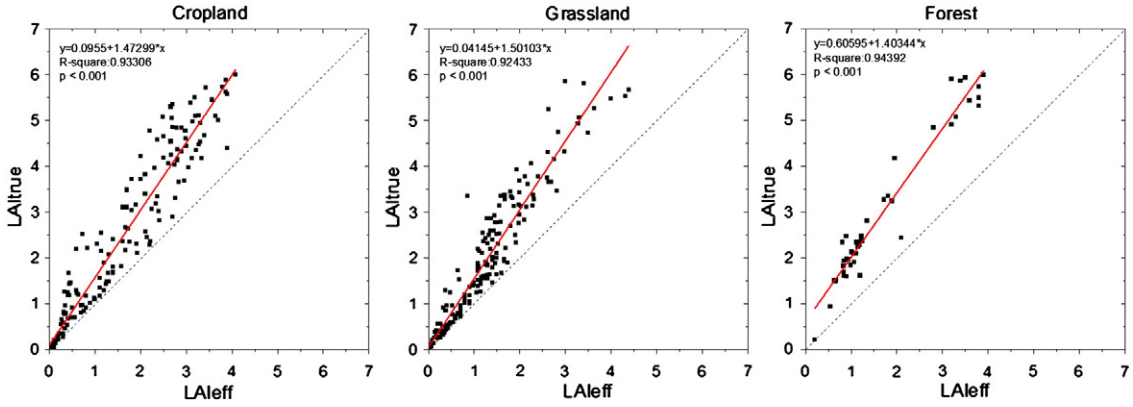

Fig. 2. Scatter plots of effective LAI and true LAI over three typical biomes.

(GCTP, WWW7) to transform SPOT/VEGETATION and MISR data (including LAI and their corresponding surface reflectance) to the MODIS projection system and to resample them with a spatial resolution of 1 km.

2.3. Construction of LAI climatology

LAI climatology is calculated as a time-smoothed mean value of the best-estimate LAI values; during the years of the observation period, poor-quality LAI values are replaced by average values. In the present research, LAI climatology served to construct the dynamic process model and to simulate reflectance under given conditions through a radiative-transfer model. This section presents the proposed process to construct LAI climatology from multiple sensors.

2.3.1. Pre-processing of LAI products from multiple sensors

The pre-processing of LAI products was based on matched LAI data from MODIS, CYCLOPES, and MISR (i.e., the same projection (ISIN) and same spatial resolution (1 km)). Thus, differences in spatial resolution were eliminated, and in addition the different temporal resolutions enabled us to enhance the time-series LAI. Finally, the quality-control flag, foliage clumping index, and filter method were applied. The result of pre-processing was a smoothed time-series LAI which combined information from MODIS, CYCLOPES, and MISR. The smoothed time-series LAI was used in the LAI climatology.

During pre-processing, a quality-control flag and a clumping index were used respectively to eliminate uncertainties due to unstable observations (Fernandes et al., 2003; Rodell et al., 2004; Shabanov et al., 2005) and the effect of foliage clumping (i.e., to convert effective LAI to true LAI) (Chen & Black, 1992; Jonckheere et al., 2004; Weiss, Baret, Garrigues, & Lacaze, 2007; Weiss et al., 2004). LAI products were categorized into high-quality LAIs (QC < 64 for MODIS LAI and SM = 0 for CYCLOPES LAI) and poor-quality LAIs (others). The MISR LAI used in this paper can be considered as of high-quality because it is summarized from the best LAI estimation of Level 2 land-surface data on the basis of an ancillary quality-assessment (QA) flag. Only high-quality LAI values were retained in the retrieved data. The gaps due to poor-quality LAIs were filled by multi-year averages. Due to the potential misrepresentation of LAI estimates, the quality-control flag was not always sufficient to restrict the analysis to high-quality LAIs (Gray & Song, 2012). This problem was addressed using Savitzky–Golay (SG) filtering to remove outliers, as will be discussed latter. Based on the extent of agreement with the assumption of a random leaf distribution over the canopy architecture, the three LAI products discussed can be categorized into true LAI (MODIS, MISR) and effective LAI (CYCLOPES). Therefore, a clumping index had to be used to convert the effective CYCLOPES LAI to true LAI values. The conversion equation is:

$$\mathrm{tLAI} = \frac{\mathrm{eLAI}}{\Omega} \tag{1}$$

where tLAI is the true LAI which takes foliage clumping into consideration, eLAI is effective LAI, and Ω is the clumping index.

Several practices have been implemented to derive global clumping indices from satellite products. Chen, Menges, and Leblanc (2005) mapped global foliage clumping using multi-angular POLDER1 (Polarization and Directionality of Earth Reflectance) data based on the Normalized Difference between Hotspot and Darkspot (NDHD). Pisek, Chen, Lacaze, Sonnentag, and Alikas (2010) extended this by integrating complete year-round observations from POLDER3 to overcome the limited number of observations from POLDER1. Pisek, Chen, and Nilson (2011) derived a clumping index from MODIS bidirectional reflectance distribution function model parameter products. Note that because the CYCLOPES LAI product corresponds to certain effective LAI products where clumping is observed only at the landscape level, it is reasonable to apply the clumping index to CYCLOPES LAI according to the specific biome type provided by MODIS Land Cover Products (MOD12). This research has used the accessible global clumping index derived from POLDER3, with a projection (SIN) analogous to MODIS (ISIN). Then the mean values of specific biomes were counted, and these statistical values were used in the proposed method. After the conversion of the

Table 2
Characteristics of LAI products and land-surface reflectance products.

Product	Satellite/sensor	Spatial resolution/coverage	Temporal resolution/span	Projection
MODIS LAI (MOD15)	Terra-Aqua/MODIS	1 km/global	8 days/2000–	ISIN
CYCLOPES LAI	SPOT/VEGETATION	1/112°(~10 km)/global	10 days/1999–2007	Plate-carrée
MISR L3 CGLS LAI	Terra/MISR	0.5°/global	1 month/2000–	GCTP_GEO
MODIS SREF (MOD09)	Terra-Aqua /MODIS	500 m/global	8 days/2000–	ISIN
SPOT S10REF	SPOT/VEGETATION	1/112°(~10 km)/global	10 days/1998–	Plate-carrée
MISR L2 BRF	Terra/MISR	1.1 km/global	1 day/2000–	SOM

MISR L3 CGLS: MISR Level 3 component global land-surface product; LAI is one of its statistical summary variables. MODIS SREF: MODIS surface reflectance product (MOD09). SPOT S10 REF: SPOT 10-day synthesized reflectance product. MISR L2BRF: MISR Level 2 bidirectional reflectance factor product.

CYCLOPES LAI, the three LAI products used could be regarded as true LAIs related to the same biome.

Subsequently, the high-quality true LAI data were used to construct an LAI climatology in which the excluded LAIs due to poor values of the quality flag were replaced by multi-year averages. Furthermore, the Savitzky–Golay (SG) filtering (Chen et al., 2004; Savitzky & Golay, 1964) was applied to capture and eliminate the subtle and rapid changes in the time series based on the assumption that LAI climatology follows annual cycles of growth and decline of vegetation. This is one of the most popular ways to analyze time-series data and has been successfully used to derive a smooth vegetation index (VI) from Advanced Very High Resolution Radiometer (AVHRR) data (Jonsson & Eklundh, 2002) and from temporally and spatially continuous MODIS LAI time series (Gao et al., 2008). After the application of SG filter, the outliers due to potential miscalculation of the quality flag were further reduced.

2.3.2. Improvement of LAI climatology

After pre-processing of LAI values from multiple satellite sensors, uncertainties due to unstable observations and foliage clumping were eliminated as much as possible. In the present research, the introduction of temporal information from three satellite sensors was able to provide higher-quality LAI values to construct LAI climatology and to narrow the interval between neighboring satellite observations.

Then this time-smoothed LAI was used to construct a dynamic model and to simulate reflectance at the given view-illumination geometry. The exact construction of the LAI climatology was one of the critical factors that contributed to retrieval accuracy. Therefore, an iteration approach was proposed to provide a better estimate of LAI climatology. The inversion result was regarded as an approximation from LAI climatology to the actual LAI, and therefore it was used to update the LAI climatology. In this way, the LAI climatology calculated from the time-smoothed mean value was improved. The root mean square error (RMSE) was used to assess performance, and as stated in Section 3, the trend of variation in RMSE was evaluated over several typical biomes in detail and demonstrated the effectiveness of this improvement.

2.4. Dynamic model based on LAI climatology

A reasonable LAI climatology can be obtained using multi-year averaging and SG filtering. However, there still exist some differences between LAI climatology and real LAI values, especially under disturbance conditions (e.g., poor atmospheric conditions). It is necessary to update the LAI when reflectance observations are available. The integration of multi-source satellite data is far more significant because of the increased number of observations and the decreased time interval between neighboring observations. In the present research, a simple dynamic model (Xiao et al., 2009, 2011) was used:

$$\mathrm{LAI}_t = F_t \times \mathrm{LAI}_{t-1} \tag{2}$$

where LAI_{t-1} means LAI at the previous time step and LAI_t means LAI at the current time step. F_t is a linear operator representing the relationship between neighboring LAI observations and can be calculated as follows:

$$F_t = 1 + \frac{1}{|\mathrm{LAIclim}_t| + \varepsilon} \times \frac{d\mathrm{LAIclim}_t}{dt} \tag{3}$$

where $\mathrm{LAIclim}_t$ is the value of LAI climatology at time step t. $\frac{d\mathrm{LAIclim}_t}{dt}$ is the first-order derivative of LAI climatology and stands for the variation tendency of LAI climatology at time step t. ε is set to 10^{-3} to avoid an invalid denominator.

2.5. Canopy radiative-transfer model

Canopy radiative-transfer models describe the relationship between canopy characteristics and reflectance. Many models have been developed to simulate canopy reflectance and to retrieve land-surface biophysical parameters from satellite observations (Kuusk, 1995a, 2009; Liang, 2004; Liang & Strahler, 1993). A two-layer canopy-reflectance model (ACRM) developed by the vegetation remote sensing group at Tartu Observatory was adopted as an inversion method in the present research. Compared with the existing multispectral CR model (MSRM) (Kuusk, 1994) and the Markov chain CR model (MCRM) (Kuusk, 1995b), the ACRM model accounts for non-Lambertian soil reflectance, the specular reflection of direct sun rays on leaves, the hotspot effect, and a two-parameter leaf-angle distribution (Kuusk, 2001). This inversion method has been widely used to estimate LAI and other biological variables from remotely sensed data and has shown excellent results (Fang & Liang, 2003a; Fang, Liang, & Kuusk, 2003; Xiao et al., 2011).

In the present study, the dynamic model construction procedure discussed earlier was used to take advantage of temporal information from the three mentioned global LAI products. The ACRM model was run to simulate reflectance at fixed wavelengths with the predicted LAI from a dynamic model and the given view-illumination geometry of satellite observations. The simulated reflectance data were then used to update the predicted LAI from the dynamic model using the ensemble Kalman filter (EnKF) technique presented in the next section. The spectral information (provided by the MODIS, SPOT/VEGETATION, and MISR surface reflectance products) and the angular information (provided by the MISR surface reflectance product) were used in the course of the EnKF technique. A detailed discussion of this information is presented in the analysis section (Section 3).

2.6. Ensemble Kalman filter

The ensemble Kalman filter is a critical sequential data-assimilation method originally proposed by Evensen (2003, 2009). It has been proven capable of efficiently handling strongly nonlinear dynamics and large state spaces and has gained in popularity because of its simple conceptual formulation and relative ease of implementation (Evensen, 1994). Here, we state the standard EnKF analytical equation expressed in terms of the ensemble covariance matrices and explain the major variables only. A detailed implementation of the EnKF method is available in the published literature of Evensen (2009):

$$A^a = A + A'A'^T H^T \left(HA'A'^T H^T + \gamma\gamma^T\right)^{-1} D' \tag{4}$$

where $A \in \Re^{n \times N}$ is defined as the matrix holding N ensemble members of n-dimensional model state vectors (i.e., four control variables and reflectance); A' is defined as the ensemble perturbation matrix; $\gamma \in \Re^{m \times N}$ is the ensemble of perturbations and its ensemble mean, equal to zero; $D' \in \Re^{n \times N}$ is the ensemble of innovation vectors; and $H \in \Re^{m \times n}$ is a linear observation operator that transforms between the augmented state vector and the observations. $A'A'^T H^T (HA'A'^T H^T + \gamma\gamma^T)^{-1}$ is the so-called Kalman gain matrix and determines to what extent the model prediction is projected onto the measurements. The superscript "a" stands for "analysis" and denotes the analyzed state-vector ensemble; the superscript "T" stands for a matrix transpose.

In the present research, four free parameters (LAI, the Markov parameter, and the weights of the first and second price functions) of ACRM, and the reflectance at several wavelengths were the elements of the ensemble members (i.e., the model state vector). In the EnKF technique, the statistical characteristics (e.g., mean value and variance) of the ensemble members can be used to represent those of the population in EnKF. The integration of high-quality time-series reflectance data and simulated reflectance values from ACRM were used to update the ensemble members (e.g., LAI). Note that in this research, the solution

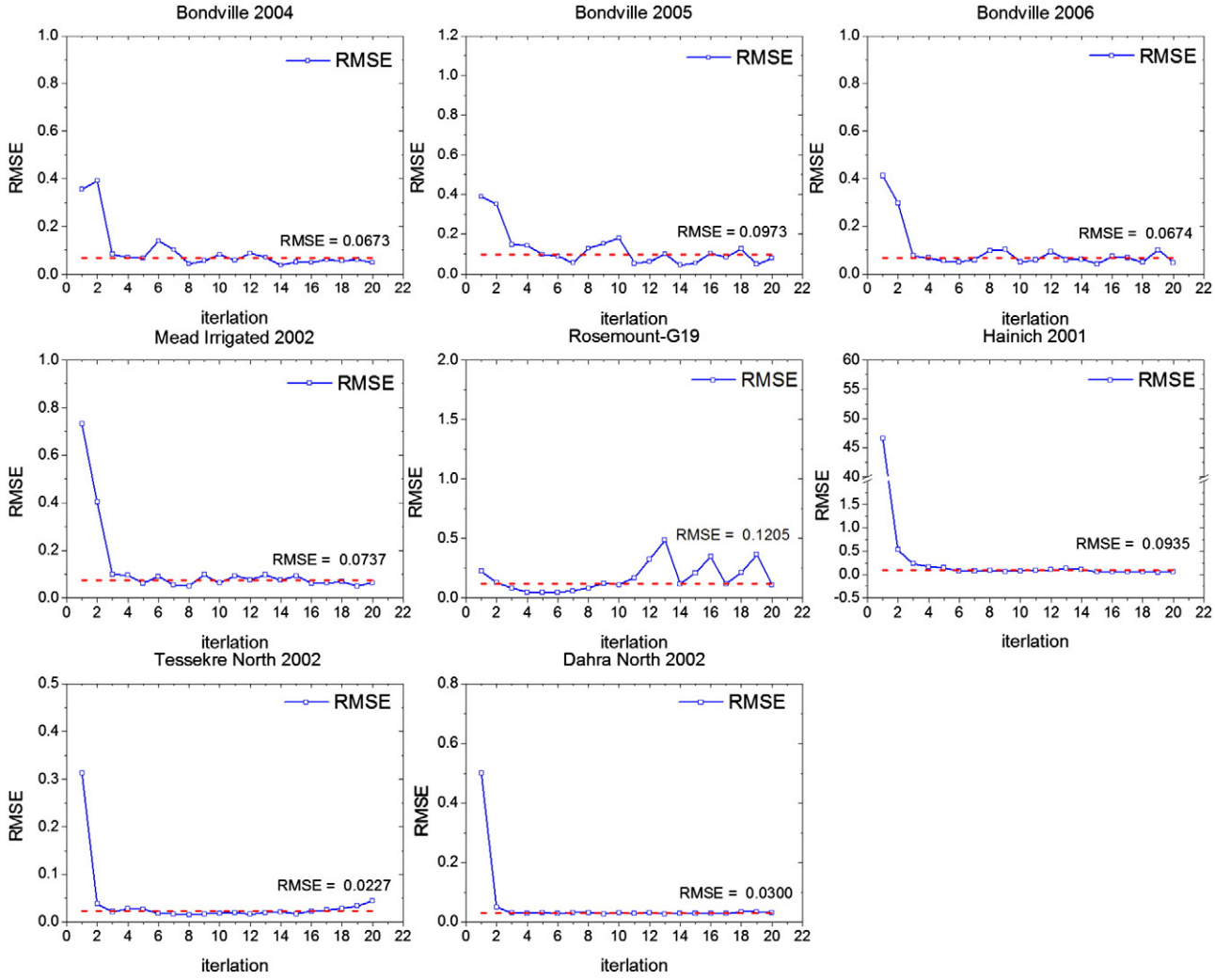

Fig. 3. Variation of RMSE (line marked with rectangles) with number of iterations.

to the ensemble members may be non-unique, despite the large quantity of surface reflectance data. In this case, the mean value of specific non-unique values was regarded as a reasonable solution to its corresponding parameters. Then the mean LAI value was used to update the LAI climatology.

2.7. The iteration process of LAI climatology

As described in Section 2.3.2, the iterative process involved using the retrieved results to update the LAI climatology to provide more accurate time-series LAI values for the dynamic model and the canopy radiative-transfer model. A key task in evaluating this procedure is to discuss the performance of the iterations and to determine explicitly its exit criteria. In this section, RMSE is used as an indicator of retrieval performance. The lines marked with rectangles (RMSE) (Fig. 3) indicate the difference between LAI climatology and retrieved LAI. In the proposed method, the retrieved LAI can be regarded as a shift from the LAI climatology to the real LAI (i.e., the actual time-series LAI of the specific site). The iteration process makes it possible to update the LAI climatology with a more accurate one; hence, when the number of iterations increases, the result

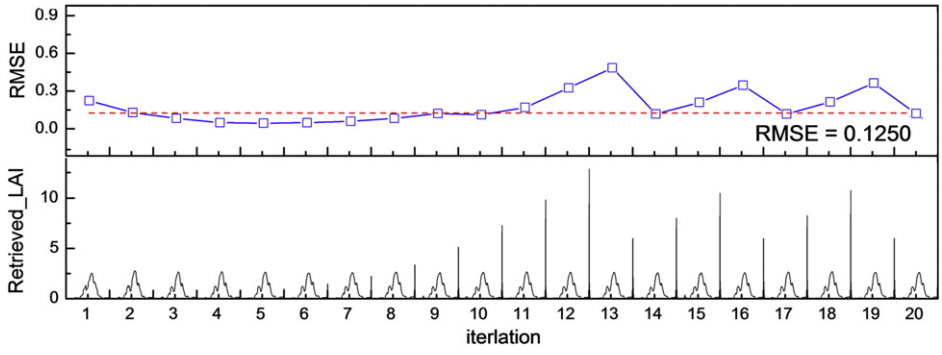

Fig. 4. Variation in RMSE and retrieved LAI with number of iterations at Rosemount-G19.

of the retrieval seems to be a closer approximation to the real LAI. Due to the latent limitations of satellite observations, model assumptions, and the clumping index, the RMSE cannot generally reach zero. In this method, a $5 * 1$ sliding window is defined to compare the RMSE of the current iteration with four surrounding ones (including two prior iterations and two subsequent iterations, all these five RMSEs being in the sliding window). If the current RMSE is the smallest, it is chosen as the minimum RMSE, and the result of the current iteration is chosen as the improved LAI; otherwise, the sliding window is moved to the next iteration to capture another five RMSEs.

To test the performance of these criteria, 20 iterations were carried out at each validation site to observe the trend of the RMSE curve. Obviously, RMSE curves for all these sites reached a relatively low value (approximately 0.1), and the minimum RMSE was easy to find in the first 10 iterations using the sliding window. Additional iterations may lead to two situations: (1) the fluctuations are not significant, which means that the extra iterations will not make much difference in the results; or (2) there is a substantial difference between certain iterations (e.g., Rosemount-G19) and the average RMSE values (the red dotted line). It is clear from Fig. 4 that the retrieved LAI values for Rosemount-G19 did not change much with number of iterations apart from the sudden rise at the beginning of the year. Therefore, iterations may improve retrieval accuracy; however, too many iterations do have the potential of exaggerating certain variations in retrieved LAI (see the unusual vertical lines at the beginning of the iterations), which also correspond to an increase in RMSE. In conclusion, the minimum RMSE approach discussed in this paper is capable of handling all the situations occurring at the validation sites.

3. Analysis of results

3.1. Assessing temporal information

One of the advantages of integrating data from multiple sensors is increasing the amount of temporal information available. In the present research, temporal information is available from the additional satellite LAI and surface reflectance data along with MODIS, SPOT/VEGETATION, and MISR data. An important task is to assess how this temporal information improves LAI estimates. Poor-quality or invalid LAI and surface reflectance data resulting from unstable observation conditions were removed on the basis of the quality-control flag during the preprocessing procedure. Then the assessment process was implemented in three steps. First, only MODIS data were used in LAI retrieval. Second, SPOT/VEGETATION data were added to the inversion. When the observation times of MODIS and SPOT/VEGETATION data coincided, only the MODIS data were kept. This ensured that when new satellite sensor data were added, the temporal information only increased. Finally, MISR data were added, coincident observations were rejected, and nadir reflectance was used only to avoid the interruption of angular information. Fig. 5 shows the procedure for including satellite data, the missing values can be inserted after quality control in terms of a single-observation system, but the multiple sensors can collect more valid LAI to enrich the details and achieve better agreement with field LAI measurements. The green bars in Fig. 5 represent available high-quality surface reflectance data. It is obvious that multiple sensors can provide more valid reflectance data, narrow the time intervals between neighboring satellite observations, and enhance data frequency for the EnKF technique. Because of the limitations of available MISR BRF data and the exclusion of coincident MISR data, the total available surface reflectance data do not change much between Fig. 5b and c.

The next step was to compare the effect of three combinations of temporal information, except for Bondville in 2004 because of the lack of MISR BRF data (Fig. 6). At the Bondville site in 2005, the missing MODIS LAI data around day 200 caused a sudden decline from day 200 in the retrievals based on MODIS data, but the results from multiple sensors could fill in the missing values and achieve better agreement

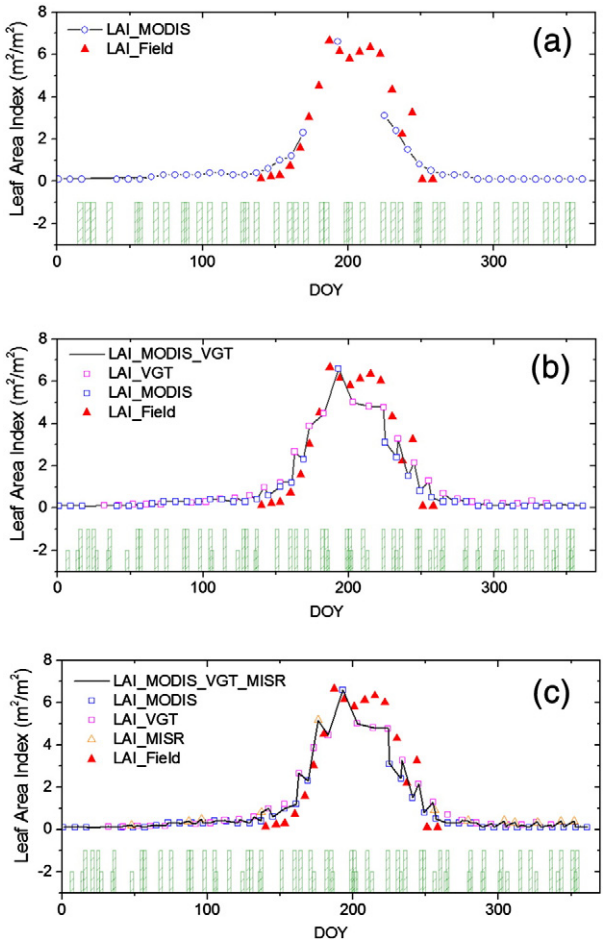

Fig. 5. Satellite data with quality control over Bondville in 2005.

with field measurements. This also occurred at other sites; inversion results based on MODIS alone (i.e., the inversion results from Xiao's method) underestimated real values to various degrees, but the inclusion of SPOT/VEGETATION and MISR data could improve the results to a relatively reasonable level. The combination of MODIS, SPOT/VEGETATION, and MISR shows the best performance during the peak of the growing season. However, there still exist some shortcomings, such as at the Mead Irrigated site. The combinations of multiple sensor data do show better performance on high values, but are not in very good agreement at the beginning of the growing season. Tessekre North and Dahra North are two sites located in Africa and covered with sparse grass savanna; the background noise is more significant than at any other sites, and the retrieved LAI values are relatively lower, with frequent fluctuations. However, the extended method proposed here also provided results which are more applicable than the retrieval results based on MODIS alone. In the proposed method, although the coincident LAI (surface reflectance) values from CYCLOPES (SPOT/VEGETATION) and MISR were removed, this never meant that the contributions from CYCLOPES (SPOT/VEGETATION) and MISR were insignificant. In other words, use of the EnKF technique was based on the existence of available satellite observations. If surface reflectance values are not available, the LAI for the next time step will be that predicted by the dynamic model. Therefore, the inclusion of time-series data with a narrowed time interval between neighbor observations enhanced the number of results from the EnKF technique (which are usually much accurate than the predictions of the dynamic model). These estimates were used in the dynamic model to provide better prediction. As a result, the incorporation of multiple sensor products can clearly lead to better results than MODIS alone.

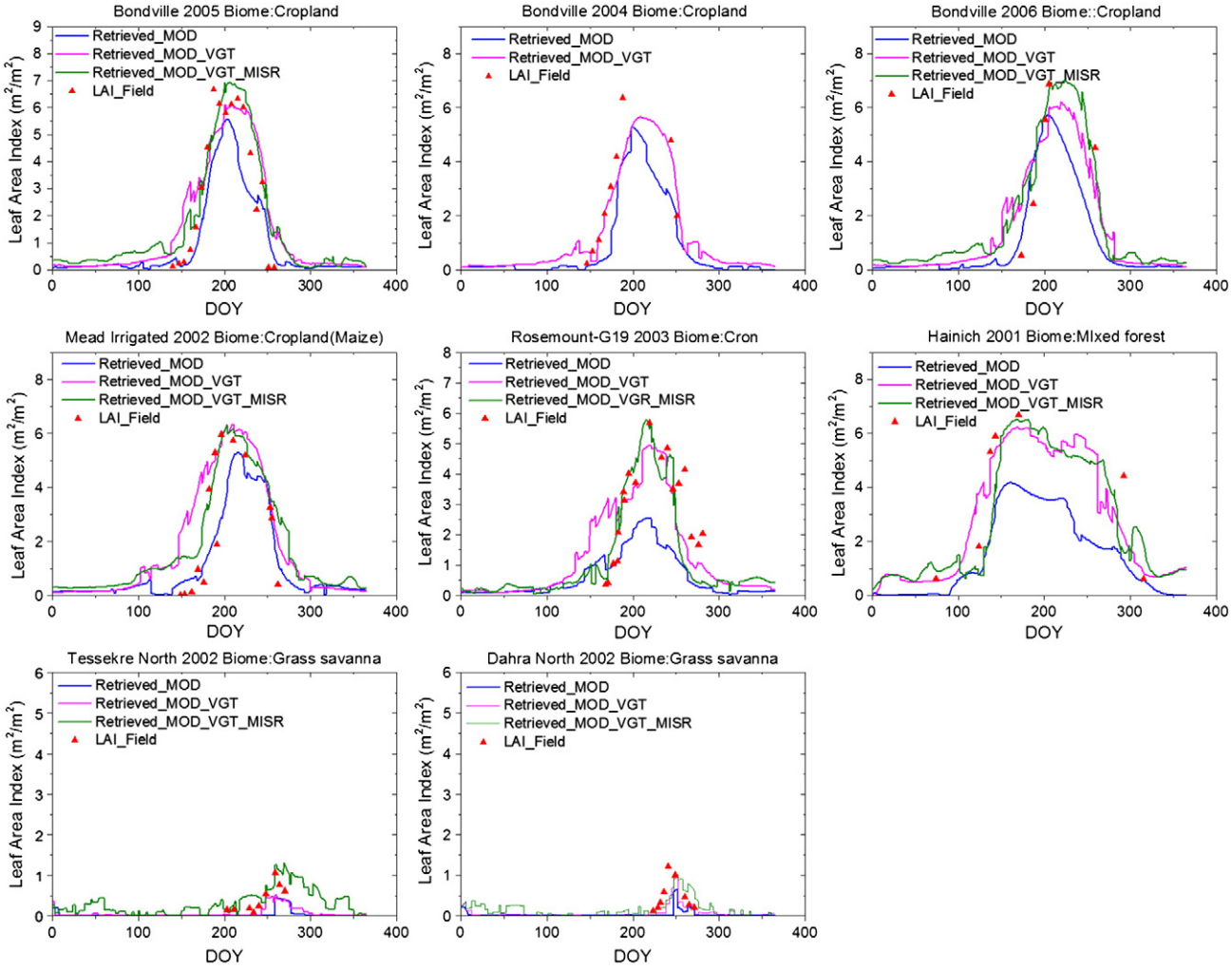

Fig. 6. Results of temporal information combinations from three sensors at six validation sites. The blue magnitude and olive lines marked as "Retrieved_MOD", "Retrieved_MOD_VGT", and "Retrieved_MOD_VGT_MISR" represent the inversion results for MODIS, MODIS + VGT, and MODIS + VGT + MISR respectively. The red triangles are field measurements from the research network.

3.2. Assessing spectral information

In the previous description, multispectral land-surface reflectance was used, and the results were acceptable compared with those derived from a single-observation system. The assessment of spectral information depends on the conclusion of Section 3.3; multiple satellite observations were used. However, reflectance in the blue and green bands is easily disturbed by poor air conditions, which may sometimes introduce error into the retrieval process. The canopy structure-sensitive red band and the near-infrared band are responsive to LAI variations. Consequently, it is an important task to assess whether spectral information improves LAI estimates. The spectral information mentioned above lies in various band combinations. The assessment was conducted in two steps. First, multispectral band reflectance from MODIS, VEGETATION, and MISR (BRF data with nadir view angle) were used for inversion. Second, the red and near-infrared bands were used to derive LAI.

Fig. 7 shows LAI values derived from multispectral bands and two specific bands (the red and near-infrared bands). Rejection of the easily disturbed blue and green bands results in better performance, especially in the beginning of the growing season. Bondville is a perfect validation site, and the retrievals achieve perfect agreement with field measurements. LAI values derived from the red and near-infrared bands improve the performance at the beginning and end of the growing season for the Mead Irrigated and Rosemount-G19 sites. Hainich contains the largest coherent area of deciduous trees in Germany. The main tree species is beech, mixed with other trees. The variation of LAI here shows a longer growing season than at other sites where the main biome is crops. The results for Tessekre North and Dahra North are quite remarkable. These two sites are located in Africa and are both covered with sparse grass savanna, and the background noise is more marked than at other sites. The exclusion of the blue and green bands was able to eliminate disturbances and led to fewer fluctuations. The comparison reveals the importance of eliminating background noise disturbances (e.g., soil, atmosphere) and highlights the information of vegetation. Reflectance of the red and near-infrared bands was demonstrated to be enough to work with the proposed extended method, but the use of easily disturbed bands will introduce additional noise. Fig. 8 shows a comparison of field measurements and LAI derived from different band combinations. LAI data derived from two bands show better agreement with field measurements ($R^2 = 0.8315$ and RMSE = 0.9327).

The conclusion of this section is also similar to that of previous studies. Kuusk (1995b) pointed out that the leaf area index of the canopy was best determined using simultaneous measurements in the red and NIR spectral regions. Fang and Liang (2003b) developed a genetic algorithm with a canopy radiative-transfer model to retrieve LAI and

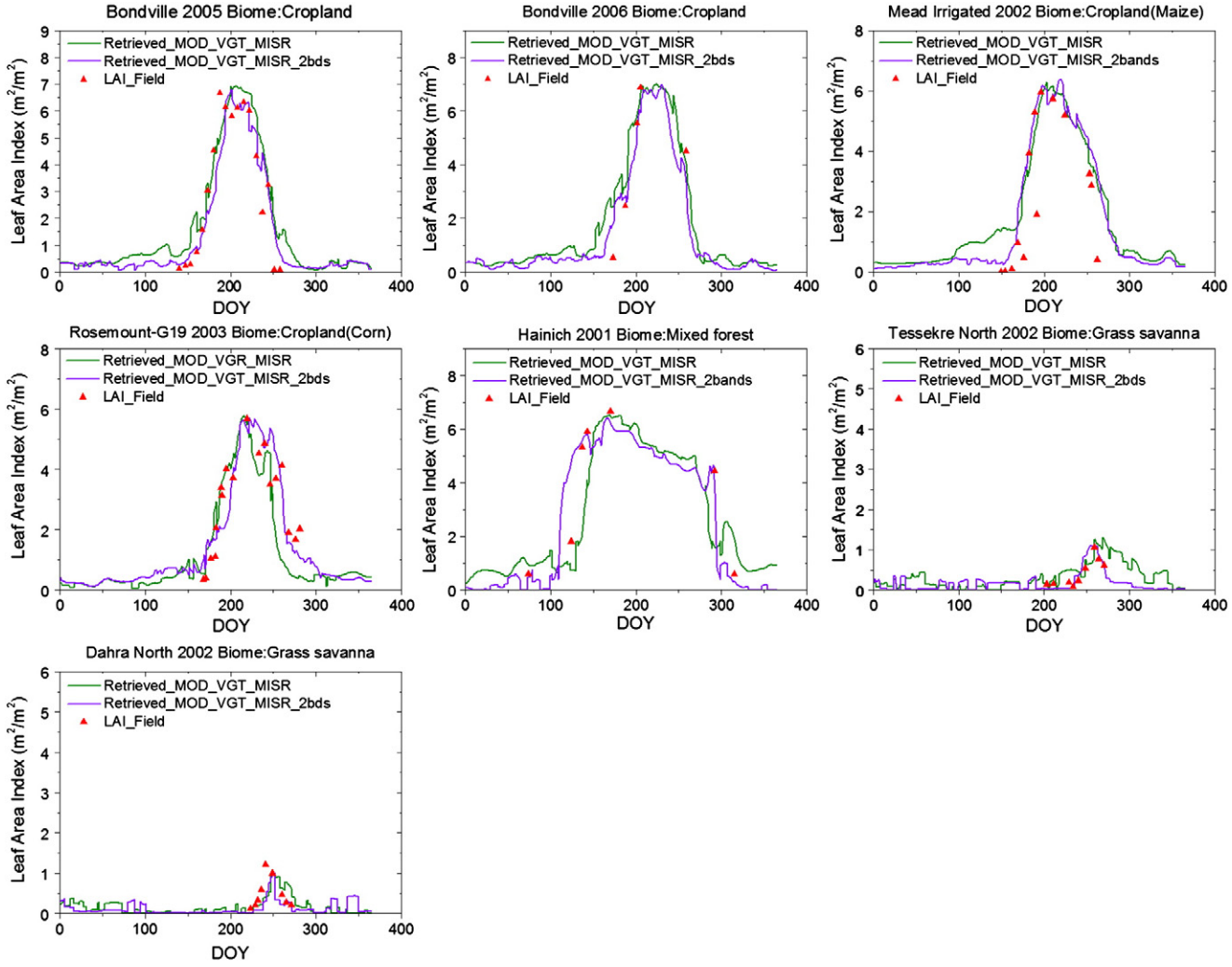

Fig. 7. Validation results for spectral information. The olive line marked as "Retrieved_MOD_VGT_MISR" represents the inversion result for multispectral bands, while the violet line marked as "Retrieved_MOD_VGT_MISR_2bds" represents the result for the red and near-infrared bands.

found that the use of red and near-infrared band reflectance provided a very good estimation of LAI. Similar results were reported by McCallum et al. (2010). The usage of red and near-infrared bands instead of multispectral bands can meet the demand of the proposed extended method and achieve better agreement with field measurements. In summary, a selection of spectral information aimed to eliminate noise from disruptive factors and to identify the sensitive bands can improve retrieval performance.

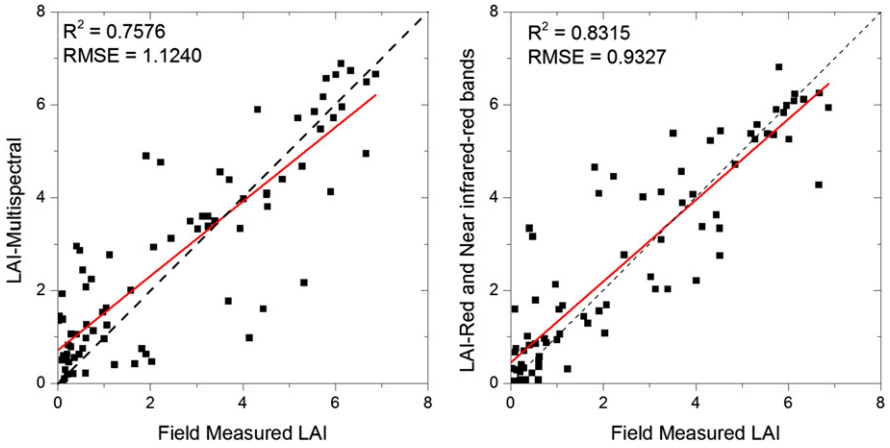

Fig. 8. Comparison of retrieved LAI with field LAI. "LAI-Multispectral" represents LAI values derived from multispectral reflectance data, while "LAI-Red and Near-infrared-red Bands" represents LAI values derived from these two specific bands.

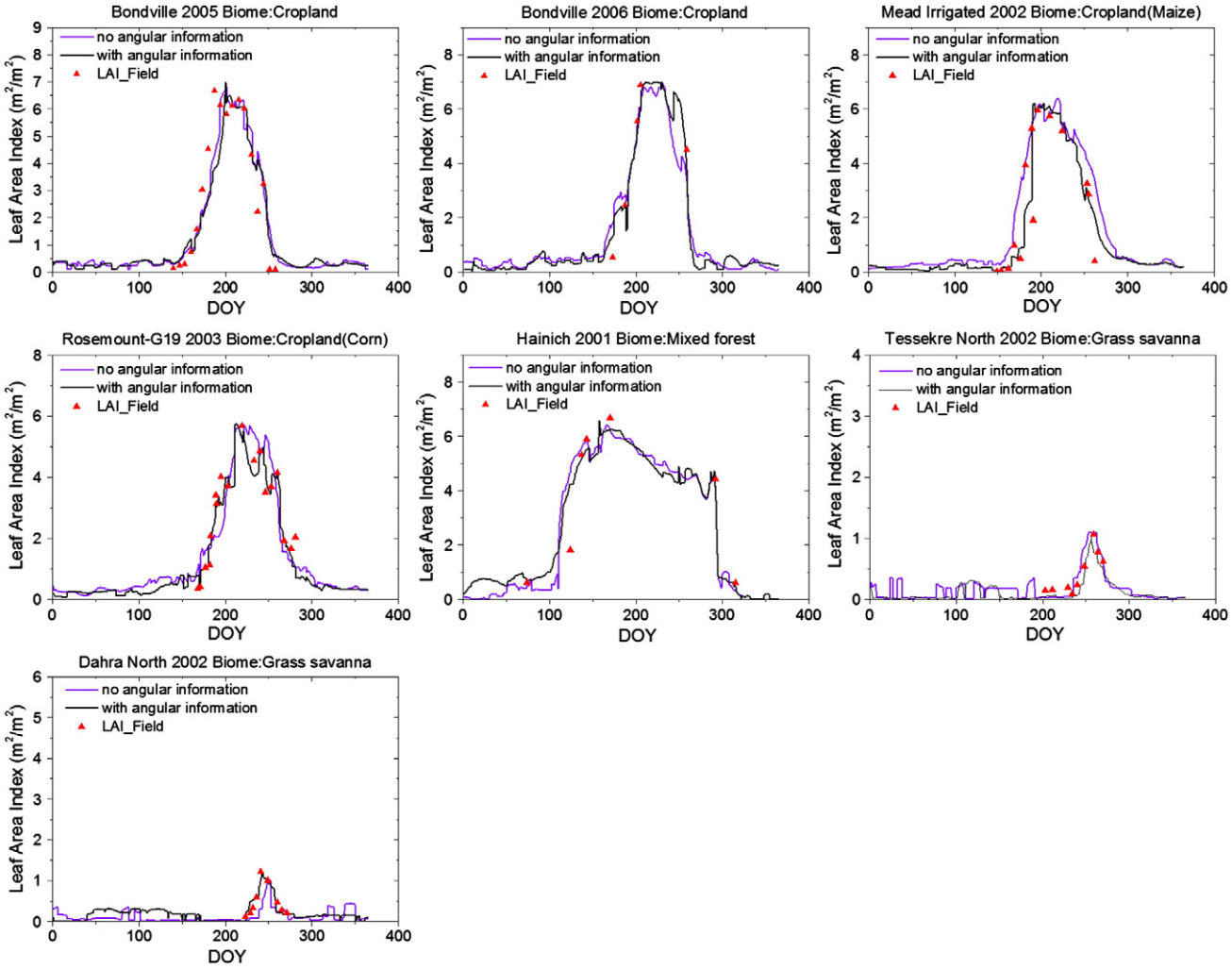

Fig. 9. Performance with additional angular information. The olive line marked as "no angular information" and the black line marked as "with angular information" represent retrievals based on combinations of angular reflectance.

3.3. Assessing angular information

MISR is a satellite sensor unlike any that has flown in space before. It is designed to provide global imagery at nine discrete viewing angles and in four visible/near-infrared spectral bands. LAI is a biophysical variable with obvious spatial structure. Therefore, it would be interesting to confirm whether the additional angular information can provide better results. Hence, a comparison test was designed to evaluate performance based on the conclusions of two previous tests. First, MODIS, Vegetation, and MISR LAI were used to construct an LAI climatology and dynamic model, and the red and near-infrared surface reflectance bands were used recursively to update the predictions of the dynamic model. Here, nadir MISR BRF data only were used. Second, MISR BRF data for an additional four neighboring observation viewing angles (−45.6°,

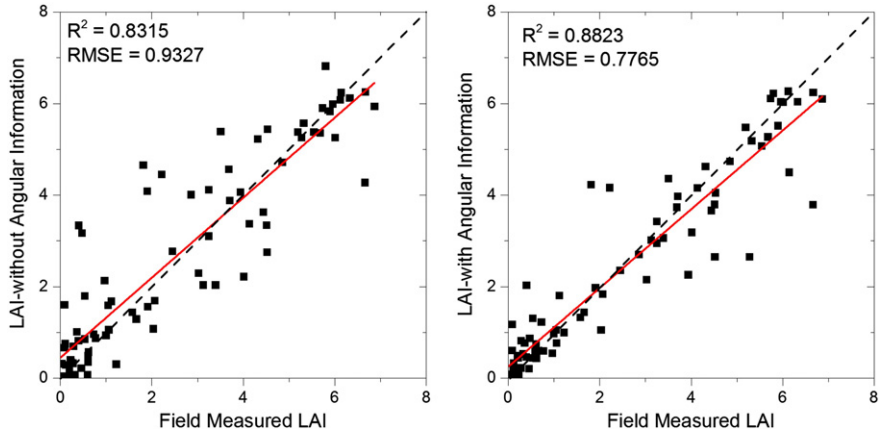

Fig. 10. Comparison of retrieved LAI with field LAI. "LAI with angular information" represents the LAI values derived with additional angular reflectance information.

−26.1°, +26.1°, and +45.6°) were used in the proposed extended method. Fig. 9 shows the performance achieved with additional angular information.

The inclusion of MISR data introduces a new type of information (i.e., angular information included in nine-directional land-surface reflectance) because of its particular mode of observation. A direct comparison was carried out to assess the angular information in the proposed extended method. Generally, Fig. 10 shows clearly that additional angular information does improve the performance of the proposed method, with R^2 increasing from 0.8315 to 0.8823 and RMSE decreasing from 0.9327 to 0.7765. Fig. 9 shows that additional angular information contributed to modest improvement on most occasions, but was not always significant. The reasonable explanation for this is the lack of valid MISR BRF data because of the specific mode of observation and unstable atmospheric conditions. For instance, very few BRF data points were available for Bondville, just one or two points after the quality-control process; this observation could also refer to Fig. 5. Only one MISR BRF data point was available for Bondville in 2005; this restricted the improvement available from additional angular information. This situation is common among other validation sites, where the number of valid BRF data points was no more than ten. Although the inclusion of additional MISR BRF viewing angles could have an effect, the lack of valid MISR BRF data restricts the opportunities for further improvement.

4. Discussion

4.1. Main contributions of the current research

The first contribution of the proposed extended method is the dynamic update of LAI climatology. An iterative method has been proposed to improve its estimation. The LAI values retrieved by the proposed extended method are regarded as an approximation of the real LAI, which is more accurate than LAI climatology. As a result, the retrieved LAI values could be substituted for LAI climatology to provide more accurate time-series LAI values. Then the proposed method recursively updates LAI by combining predictions from a dynamic model with high-quality land-surface reflectance data from three satellites. In Section 2.7, the variations in RMSE between retrieved LAI and LAI climatology were analyzed. The decline of RMSE at the beginning of the iterations meant that LAI climatology values were approaching the retrieved LAI. Then, the RMSE continued to fluctuate with a small magnitude; this indicates that further updates of LAI climatology would not make a significant difference. However, the continued iterations might have exaggerated certain variations in the retrieved data (e.g., Rosemout-G19 site, see Fig. 4). In conclusion, a $5 * 1$ sliding window was defined to determine the minimum RMSE value, and the corresponding retrieved LAI was regarded as the best estimate from our proposed method.

Besides the dynamic update of LAI climatology, another contribution of this study is the integration of data from multiple sensors with different spectral, spatial, temporal, and angular information to reveal the best combination of remotely sensed information. It is now an important research challenge to solve the ill-posed problem of estimating land-surface variables from remote sensing data (Liang & Qin, 2008). LAI data from multiple sensors have been used to fill the gaps due to the limited information from single-observation systems to produce better estimates of LAI climatology. The additional satellite reflectance is able to narrow the time intervals between neighboring steps in the EnKF technique. The performance of temporal, spectral, and angular information was assessed in Section 3, and the results demonstrate that the integration of MODIS, SPOT/VEGETATION, and MISR data produced better LAI estimates than any one or two sources. In addition, LAI estimation with reflectance in red and near-infrared bands works better than those with multispectral bands. The introduction of MISR angular information could also contribute to further improvement of the estimates, but is restricted by the scarcity of valid data. Obviously, all the evidence points to the conclusion that the integration of multi-sensor LAI (i.e., based on MODIS, SPOT/VEGETATION, and MISR), corresponding red and near-infrared reflectance, and multi-angular MISR information is the best way to retrieve LAI using the proposed new method.

4.2. Limitations of this study

The method proposed here has taken advantage of routinely produced satellite data to provide better LAI estimation. However, there still exist several limitations which need to be mentioned.

The first limitation is related to the satellite data themselves, which are constrained by instabilities in observation such as calibration errors, atmospheric, cloud contamination, view-illumination geometry effects, and saturation of reflectance in dense canopies. Moreover, the quality flags accompanying the LAI and surface reflectance products do not infallibly identify their quality. Although we have tried our utmost to address these problems, some errors may still exist.

The second limitation is the elimination of the effect of the foliage clumping index. In our study, the clumping index is restricted to the POLDER observation cycle, and the CYCLOPES LAI is not an absolutely effective estimate because it considers the clumping representation at landscape scale. There still exist some uncertainties in the conversion from effective LAI to true LAI based on the statistical mean values of specific biomes. Use of the higher-resolution clumping index derived from MODIS BRDF products (if available) will be addressed in further research.

The last limitation is the representation of biomes in the validation section. To test the performance of the retrieved LAI effectively, sites with more measurements during single years are needed. Consequently, the small number of available sites for this research leads to limited representation of certain vegetation biomes, especially forest. Moreover, the field-measured LAI values collected from existing research networks are each the mean value of several discrete sampled values. Certain errors associated with scale effect still exist, although various sampling methods have been proposed. The ideal LAI data used to validate the retrieved LAI should be derived from high resolution imagery. This topic will be explored in future research.

5. Conclusions

The pressing need for land-surface ecosystems modeling and environmental monitoring has led to a demand for high-quality, long-term consistent LAI products. However, currently available global LAI products may not meet the requirements from the viewpoint of accuracy and consistency. LAI gaps due to various reasons also impose restrictions on the further application of data. In the method proposed here, an existing inversion scheme was extended to integrate MODIS, SPOT/VEGETATION, and MISR data and to take advantage of temporal, spectral and angular information. To ensure good inversion performance, a quality flag layer and an SG filter were used to eliminate uncertainties due to unstable satellite observations and to produce a relatively smooth LAI seasonal-variation curve (i.e., LAI climatology). A clumping index based on POLDER was used to convert effective LAI to true LAI. Validation sites from several typical biomes were used to test the applicability of the proposed method. An iterative method was also proposed to perfect the estimation of LAI climatology and was demonstrated to be effective. Furthermore, three progressive tests were carried out to assess the performance of temporal, spectral, and angular information.

In summary, temporal information is indeed vital. The involvement of MODIS, SPOT/VEGETATION, and MISR data can provide more valid LAI observations to improve the specification of change tendencies and to construct a better LAI climatology. Moreover, the additional surface reflectance information can narrow the time intervals and thereby increase the number of results which are updated by the EnKF technique. The rejection of easily disturbed reflectance bands (i.e., blue and green bands) can avoid errors from the atmosphere and other

factors. MISR multi-angular information is capable of representing spatially structured LAI data, although it is also restricted by the limited number of available MISR BRF data points. All these results show the potential to achieve better retrieval than with a single sensor. The validations over the six sites are consistent with the above explanation. Temporal information from MODIS, Vegetation, and MISR data, spectral information from red and near-infrared bands, and angular information from MISR BRF data are the best combination of remotely sensed information to obtain the best estimated LAI using the proposed extended method.

Acknowledgments

This research was supported by the National Natural Science Foundation of China (NSFC) under grants 41331173 and 41171264, and the National High Technology Research and Development Program of China via Grant 2013AA122801. We are indebted to many investigators and to FluxNet (WWW5), AmeriFlux (WWW6), Bigfoot (Cohen & Justice, 1999), and VALERI (WWW7) for providing the other field measurement data.

References

Bacour, C., Baret, F., Béal, D., Weiss, M., & Pavageau, K. (2006). Neural network estimation of LAI, fAPAR, fCover and LAI × Cab, from top of canopy MERIS reflectance data: Principles and validation. *Remote Sensing of Environment*, *105*, 313–325.

Baret, F., & Guyot, G. (1991). Potentials and limits of vegetation indices for LAI and FAPAR assessment. *Remote Sensing of Environment*, *35*, 161–173.

Baret, F., Hagolle, O., Geiger, B., Bicheron, P., Miras, B., Huc, M., et al. (2007). LAI, fAPAR and fCover CYCLOPES global products derived from VEGETATION Part 1: Principles of the algorithm. *Remote Sensing of Environment*, *110*, 275–286.

Baret, F., Weiss, M., Allard, D., Garrigues, S., Leroy, M., Jeanjean, H., et al. (2005). *VALERI: A network of sites and a methodology for the validation of medium spatial resolution land satellite products.* http://w3.avignon.inra.fr/valeri/documents/VALERI-RSESubmitted.pdf (accessed 12 Feb 2014).

Bonan, G. B. (1995). Land-atmospheric interactions for climate system models: Coupling biophysical, biogeochemical and ecosystem dynamical processes. *Remote Sensing of Environment*, *51*, 57–73.

Buermann, W., Dong, J., Zeng, X., Myneni, R. B., & Dickinson, R. E. (2001). Evaluation of the utility of satellite-based vegetation leaf area index data for climate simulations. *Journal of Climate*, *14*, 3536–3550.

Chen, J. M., & Black, T. (1992). Defining leaf area index for non-flat leaves. *Plant, Cell & Environment*, *15*, 421–429.

Chen, J., Jönsson, P., Tamura, M., Gu, Z., Matsushita, B., & Eklundh, L. (2004). A simple method for reconstructing a high-quality NDVI time-series data set based on the Savitzky–Golay filter. *Remote Sensing of Environment*, *91*, 332–344.

Chen, J., Menges, C., & Leblanc, S. (2005). Global mapping of foliage clumping index using multi-angular satellite data. *Remote Sensing of Environment*, *97*, 447–457.

Cohen, W. B., & Justice, C. O. (1999). Validating MODIS terrestrial ecology products linking in situ and satellite measurements. *Remote Sensing of Environment*, *70*, 1–3.

Combal, B., Baret, F., Weiss, M., Trubuil, A., Mace, D., Pragnere, A., Myneni, R., & Knyazikhin, Y. (2002). Wang, L. *Retrieval of canopy biophysical variables from bidirectional reflectance using prior information to solve the ill-posed inverse problem. Remote Sensing of Environment*, *84*, 1–15.

Deng, F., Chen, J. M., Plummer, S., Chen, M., & Pisek, J. (2006). Global LAI algorithm integrating the bidirectional information. *IEEE Transactions on Geoscience and Remote Sensing*, *44*, 2219–2229.

Dickinson, R. (1995). Land–atmosphere interaction. *Review of Geophysics*, *33*, 917–922.

Diner, D. J., Martonchik, J. V., Borel, C., Gerstl, S. A., Gordon, H. R., Knyazikhin, Y., et al. (1999). *Level 2 surface retrieval algorithm theoretical basis.* Jet Propulsion Laboratory, California Institute of Technology, 1–81.

Evensen, G. (1994). Sequential data assimilation with a non-linear quasi-geostrophic model using Monte Carlo methods to forecast error statistics. *Journal of Geophysical Research*, *99*, 10,143–110,162.

Evensen, G. (2003). The ensemble Kalman filter: Theoretical formulation and practical implementation. *Ocean Dynamics*, *53*, 343–367.

Evensen, G. (2009). *Data assimilation: The ensemble Kalman filter.* Dordrecht Heidelberg London New York: Springer.

Fang, H., & Liang, S. (2003). Retrieve LAI from Landsat 7 ETM + data with a neural network method: Simulation and validation study. *IEEE Transactions on Geoscience and Remote Sensing*, *41*, 2052–2062.

Fang, H., & Liang, S. (2003). Retrieving leaf area index with a neural network method: simulation and validation. *IEEE Transactions on Geoscience and Remote Sensing*, *41*, 2052–2062.

Fang, H., Liang, S., & Kuusk, A. (2003). Retrieving leaf area index using a genetic algorithm with a canopy radiative transfer model. *Remote Sensing of Environment*, *85*, 257–270.

Fang, H., Wei, S., & Liang, S. (2012). Validation of MODIS and CYCLOPES LAI products using global field measurement data. *Remote Sensing of Environment*, *119*, 43–54.

Fernandes, R. A., Butson, C., Leblanc, S., & Latifovic, R. (2003). A Landsat-5 TM and Landsat-7ETM + based accuracy assessment of leaf area index products for Canada derived from SPOT4/VGT data. *Canadian Journal of Remote Sensing*, *29*, 241–258.

Ganguly, S., Schull, M., Samanta, A., Shabanov, N., Milesi, C., Nemani, R., et al. (2008). Generating vegetation leaf area index earth system data record from multiple sensors. Part 1: Theory. *Remote Sensing of Environment*, *112*, 4333–4343.

Gao, F., Morisette, J. T., Wolfe, R. E., Ederer, G., Pedelty, J., Masuoka, E., et al. (2008). An algorithm to produce temporally and spatially continuous MODIS-LAI time series. *IEEE Geoscience and Remote Sensing Letters*, *5*, 60–64.

García-Haro, F. J., Coca, F. C. -d, & Miralles, J. M. (2008). Inter-Comparision of SEVIRI/MSG and MERIS/ENVISAT Biophysical Products over Europe and Africa. *Proc. of the '2nd MERIS/(A)ATSR User Workshop* (ESA Communication Production Office, European Space Agency, Noordwijk, The Netherlands).

Garrigues, S., Lacaze, R., Baret, F., Morisette, J. T., Weiss, M., Nickeson, J. E., et al. (2008). Validation and intercomparison of global leaf area index products derived from remote sensing data. *Journal of Geophysical Research*, *113*.

Garrigues, S., Shabanov, N. V., Swanson, K., Morisette, J. T., Baret, F., & Myneni, R. B. (2008). Intercomparison and sensitivity analysis of leaf area index retrievals from LAI-2000, AccuPAR, and digital hemispherical photography over croplands. *Agricultural and Forest Meteorology*, *148*, 1193–1209.

GCOS (2006). *Systematic observation requirements for satellite-based products for climate.* (Geneva, Switzerland).

Gonsamo, A., & Chen, J. M. (2014). Improved LAI algorithm implementation to MODIS data by incorporating background, topography, and foliage clumping information. *IEEE Transactions on Geoscience and Remote Sensing* 52, 1076–1088.

Gray, J., & Song, C. (2012). Mapping leaf area index using spatial, spectral, and temporal information from multiple sensors. *Remote Sensing of Environment*, *119*, 173–183.

GTOS (2007). Further progress in the development of guidance materials, standards and reporting guidelines for terrestrial observing systems for climate. *Assessing the status of the development of standards for the essential climate variables in the terrestrial domain* (pp. 1–47) (Bali).

Hu, J., Su, Y., Tan, B., Huang, D., Yang, W., Schull, M., et al. (2007). Analysis of the MISR LAI/FPAR product for spatial and temporal coverage accuracy and consistency. *Remote Sensing of Environment*, *107*, 334–347.

Jonckheere, I., Fleck, S., Nackaerts, K., Muys, B., Coppin, P., Weiss, M., et al. (2004). Review of methods for in situ leaf area index determination Part I. Theories, sensors and hemispherical photography. *Agricultural and Forest Meteorology*, *121*, 19–35.

Jonsson, P., & Eklundh, L. (2002). Seasonality extraction by function fitting to time-series of satellite sensor data. *IEEE Transactions on Geoscience and Remote Sensing*, *40*, 1824–1832.

Knyazikhin, Y., Martonchik, J. V., Myneni, R. B., Diner, D. J., & Running, S. W. (1998). Synergistic algorithm for estimating vegetation canopy leaf area index and fraction of absorbed photosynthetically active radiation from MODIS and MISR data. *Journal of Geophysical Research*, *103*, 32,257–232,276.

Koetz, B., Baret, F., Poilvé, H., & Hill, J. (2005). Use of coupled canopy structure dynamic and radiative transfer models to estimate biophysical canopy characteristics. *Remote Sensing of Environment*, *95*, 115–124.

Kuusk, A. (1994). A multispectral canopy reflectance model. *Remote Sensing of Environment*, *50*, 75–82.

Kuusk, A. (1995). A fast, invertible canopy reflectance model. *Remote Sensing of Environment*, *51*, 342–350.

Kuusk, A. (1995). A Markov chain model of canopy reflectance. *Agricultural and Forest Meteorology*, *76*, 221–236.

Kuusk, A. (2001). A two-layer canopy reflectance model. *Journal of Quantitative Spectroscopy and Radiative Transfer*, *71*, 1–9.

Kuusk, A. (2009). Two-layer canopy reflectance model ACRM user guide. Tartu Observatory.

Liang, S. (2004). *Quantitative remote sensing of land surfaces.* John Wiley and Sons, Inc.

Liang, S. (2007). Recent developments in estimating land surface biogeophysical variables from optical remote sensing. *Progress in Physical Geography*, *31*, 501–516.

Liang, S., & Qin, J. (2008). Data assimilation methods for land surface variable estimation. In S. Liang (Ed.), *Advances in land remote sensing: System, modeling, inversion and applications* (pp. 313–339). New York: Springer.

Liang, S., & Strahler, A. H. (1993). An analytic BRDF model of canopy radiative transfer and its inversion. *IEEE Transactions on Geoscience and Remote Sensing*, *5*, 1081–1092.

Los, S. O., Collatz, G. J., Sellers, P. J., Malmstroem, C. M., Pollack, N. H., DeFries, R. S., et al. (2000). A global 9-yr biophysical land surface dataset from NOAA AVHRR data. *Journal of Hydrometeorology*, *1*, 183–199.

Masson, V., Champeaux, J. L., Chauvin, F., Meriguer, C., & Lacaze, R. (2003). A global database of land surface parameters at 1-km resolution in meteorological and climate models. *Journal of Climate*, *16*, 1261–1282.

McCallum, I., Wagner, W., Schmullius, C., Shvidenko, A., Obersteiner, M., Fritz, S., et al. (2010). Comparison of four global FAPAR datasets over Northern Eurasia for the year 2000. *Remote Sensing of Environment*, *114*, 941–949.

Myneni, R. B., Hall, F. G., Sellers, P. J., & Marshak, A. L. (1995). The interpretation of spectral vegetation indices. *IEEE Transactions on Geoscience and Remote Sensing*, *33*, 481–486.

Myneni, R. B., Nemani, R. R., & Running, S. W. (1997). Estimation of global leaf area index and absorbed par using radiative transfer models. *IEEE Transactions on Geoscience and Remote Sensing*, *35*, 1380–1393.

Nouvellon, Y., Rambal, S., Lo Seen, D., Moran, M. S., Lhomme, J. P., & Bégué, A. (2000). Modelling of daily fluxes of water and carbon from shortgrass steppes. *Agricultural and Forest Meteorology*, *100*, 137–153.

Pisek, J., Chen, J. M., Lacaze, R., Sonnentag, O., & Alikas, K. (2010). Expanding global mapping of the foliage clumping index with multi-angular POLDER three measurements: Evaluation and topographic compensation. *ISPRS Journal of Photogrammetry and Remote Sensing*, *65*, 341–346.

Pisek, J., Chen, J. M., & Nilson, T. (2011). Estimation of vegetation clumping index using MODIS BRDF data. *International Journal of Remote Sensing*, *32*, 2645–2657.
Rodell, M., Houser, P. R., Jambor, U., Gottschalck, J., Mitchell, K., Meng, C. J., et al. (2004). The global land data assimilation system. *Bulletin of the American Meteorological Society*, *85*, 381–394.
Roujean, J. -L., & Lacaze, R. (2002). Global mapping of vegetation parameters from POLDER multiangular measurements for studies of surface-atmosphere interactions: A pragmatic method and its validation. *Journal of Geophysical Research*, *107*, 4150–4160.
Running, S. W., Baldocchi, D., Turner, D. P., Gower, S. T., Bakwin, P.S., & Hibbard, K. A. (1999). A global terrestrial monitoring network integrating tower fluxes, flask sampling, ecosystem modeling and EOS satellite data. *Remote Sensing of Environment*, *70*, 108–127.
Savitzky, A., & Golay, M. J. (1964). Smoothing and differentiation of data by simplified least squares procedures. *Analytical Chemistry*, *36*, 1627–1639.
Sellers, P. J., Dickinson, R. E., Randall, D. A., Betts, A. K., Hall, F. G., Berry, J. A., et al. (1997). Modeling the exchange of energy, water, and carbon between continents and atmosphere. *Science*, *275*, 602–609.
Sellers, P. J., Los, S. O., Tucker, C. J., Justice, C. O., Dazlich, D. A., Collatz, G. J., et al. (1996). A revised land surface parameterization (SiB2) for atmospheric GCMS Part II: The generation of global fields of terrestrial biophysical parameters from satellite data. *Journal of Climate*, *9*, 706–737.
Shabanov, N. V., Huang, D., Yang, W., Tan, B., Knyazikhin, Y., Myneni, R. B., et al. (2005). Analysis and optimization of the MODIS leaf area index algorithm retrievals over broadleaf forests. *IEEE Transactions on Geoscience and Remote Sensing*, *43*, 1855–1865.
Walthalla, C., Dulaneya, W., Anderson, M., Norman, J., Fang, H., & Liang, S. (2004). A comparison of empirical and neural network approaches for estimating corn and soybean leaf area index from Landsat ETM + imagery. *Remote Sensing of Environment*, *92*, 465–474.
Wang, D. (2012). High-level Land product integration methods. In S. Liang, X. Li, & J. Wang (Eds.), *Advanced remote sensing terrestrial information extraction and applications* (pp. 667–690). Academic Press.
Wang, F., Huang, J., Tang, Y., & Wang, X. (2007). New vegetation index and its application in estimating leaf area index of rice. *Rice Science*, *14*, 195–203.
Weiss, M., Baret, F., Garrigues, S., & Lacaze, R. (2007). LAI and fAPAR CYCLOPES global products derived from VEGETATION. Part 2: validation and comparison with MODIS collection 4 products. *Remote Sensing of Environment*, *110*, 317–331.
Weiss, M., Baret, F., Smith, G. J., Jonckheere, I., & Coppin, P. (2004). Review of methods for in situ leaf area index (LAI) determination Part II. Estimation of LAI, errors and sampling. *Agricultural and Forest Meteorology*, *121*, 37–53.
Xiao, Z. (2012). Compositing, smoothing, and gap-filling techniques. In S. Liang, X. Li, & J. Wang (Eds.), *Advanced remote sensing terrestrial information extraction and applications* (pp. 75–90). Academic Press.
Xiao, Z., Liang, S., Wang, J., Chen, P., Yin, X., Zhang, L., et al. (2013). Use of general regression neural networks for generating the GLASS leaf area index product from time series MODIS surface reflectance. *IEEE Transactions on Geoscience and Remote Sensing*, 1–15.
Xiao, Z., Liang, S., Wang, J., & Jiang, B. (2011). Real-time inversion of leaf area index from MODIS time series data. *Remote Sensing of Environment*, *115*, 97–106.
Xiao, Z., Liang, S., Wang, J., Song, J., & Wu, X. (2009). A temporally integrated inversion method for estimating leaf area index from MODIS data. *IEEE Transactions on Geoscience and Remote Sensing*, *47*, 2536–2545.
Yang, W., Tan, B., Huang, D., Rautiainen, M., Shabanov, N. V., Wang, Y., et al. (2006). MODIS leaf area index products from validation to algorithm improvement. *IEEE Transactions on Geoscience and Remote Sensing*, *44*, 1885–1898.
Zhang, P., Anderson, B., Tan, B., Huang, D., & Myneni, R. (2005). Potential monitoring of crop production using a satellite-based Climate-Variability Impact Index. *Agricultural and Forest Meteorology*, *132*, 344–358.

WWW Sites

WWW1. The FLUXNET database. http://www.fluxnet.ornl.gov/
WWW2. AmeriFlux site and data exploration system. http://ameriflux.ornl.gov/
WWW3. Validation of Land European Remote Sensing Instruments. http://w3.avignon.inra.fr/valeri/
WWW4. Warehouse inventory search tool (WIST). http://wist.echo.nasa.gov/
WWW5. PÔle d'Observation des Surfaces continentales par TELédétection. http://postel.mediasfrance.org/
WWW6. MISR Home Page. www.misr.jpl.nasa.gov/
WWW7. General Cartographic Transformation Package software (GCTP). http://gcmd.nasa.gov/records/USGS-GCTP.html